

Barking Up The Syntactic Tree: Enhancing VLM Training with Syntactic Losses

Jiayun Luo[#], Mir Rayat Imtiaz Hossain[#], Boyang Li^b, and Leonid Sigal[#]

[#]University of British Columbia, Vector Institute for AI, Canada

^bNanyang Technological University, Singapore

{letitlal, rayat137, lsigal}@cs.ubc.ca, {boyang.li}@ntu.edu.sg

Abstract

Vision-Language Models (VLMs) achieved strong performance on a variety of tasks (e.g., image-text retrieval, visual question answering). However, most VLMs rely on coarse-grained image-caption pairs for alignment, relying on data volume to resolve ambiguities and ground linguistic concepts in images. The richer semantic and syntactic structure within text is largely overlooked. To address this, we propose Hierarchically Structured Learning (HIST) that enhances VLM training without any additional supervision, by hierarchically decomposing captions into the constituent Subject, Noun Phrases, and Composite Phrases. Entailment between these constituent components allows us to formulate additional regularization constraints on the VLM attention maps. Specifically, we introduce two novel loss functions: (1) Subject Loss, which aligns image content with the subject of corresponding phrase, acting as an entailment of standard contrastive/matching losses at the Phrase level; (2) Addition Loss, to balance attention across multiple objects. HIST is general, and can be applied to any VLM for which attention between vision and language can be computed; we illustrate its efficacy on BLIP and ALBEF. HIST outperforms baseline VLMs, achieving up to +9.8% improvement in visual grounding, +6.3% in multi-object referring segmentation, +1.1% in image-text retrieval, and +0.2% in visual question answering, underscoring the value of structuring learning in VLMs.

1. Introduction

Vision-Language Models (VLMs) [2, 15, 18, 23, 25–27, 29, 33, 37, 44], pretrained on vast amounts of image-text pairs, generalize effectively across a wide variety of downstream tasks, including image-text retrieval [28, 31], visual question answering [11], and visual grounding [17, 46]. However, VLMs primarily leverage a direct, coarse-grained alignment between image and caption pairs, often overlooking the deeper structures embedded in the textual data.

Historically, the natural language processing (NLP) has

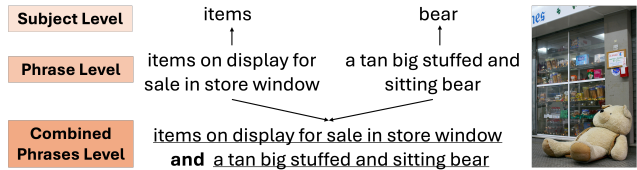


Figure 1. **Motivation.** Existing VLM models train from image-caption pairs, requiring large corpora of data to establish word-region associations. The proposed Hierarchically Structured (HIST) learning framework, and associated losses, through syntactic analysis, decompose captions into hierarchy of noun phrases establishing entailment between them and the image and among the phrases themselves. Specifically, it extracts nouns (*Subject level*) from noun phrases and aligns them to the image, along with the corresponding noun phrases themselves (*Noun Phrase level*). In addition, it combines two noun phrases together into longer composite phrases and regularizes attention to be a sum of the constituent noun sub-phrases (*Composite Combined Phrase level*).

made significant progress in understanding textual structure through the development of various parsing methods. Techniques such as syntactic parsing [30, 32], which decomposes sentences into hierarchical syntax trees, have been instrumental in identifying linguistic patterns and relationships between words [32]. These methods reveal the internal structure of text, allowing models to better capture the semantics within a sentence. Parsing has been effectively utilized in numerous tasks such as machine translation [3, 10] and sentence classification [20, 41], where understanding the hierarchical relationships in text provides substantial gains in accuracy. Syntactic parsing has also been shown to be useful in image-text retrieval [40], with order embeddings, and visual grounding [42]; preceding recent advances in LLMs and VLMs. However, such efforts have largely been abandoned more recently. Their efficacy and the general question of how richer textual representations can benefit VLM training remains open.

To this end, we propose a novel Hierarchically Structured (HIST) learning framework that strengthens the connection between vision and language by embedding hierarchical text structures into the training process, without

requiring annotation beyond image-text pairs. Our framework decomposes captions into noun phrases, each focusing on a distinct object within the image, and organizes these phrases into a three-level hierarchy: *Subject Level*, *Noun Phrase Level*, and *Composite Combined Phrase Level*, as depicted in Figure 1. The Combined Phrase level serves as the root, formed by joining two object-centric phrases using an “and”¹. The object-centric phrases themselves are represented at the (middle) Noun Phrase level. Finally, the parsed subject of each noun phrase form the Subject level and the leaf of the syntactic hierarchy.

Entailment between these constituent components of the sentence and the image, allows us to formulate additional regularization constraints for training of VLMs. Specifically, we leverage three losses. At the *Phrase Level* we ensure alignment (entailment) between noun phrases and the image by leveraging standard VLM losses typically applied for image-caption pairs: image-text contrastive (ITC), image-text matching (ITM), and masked language modeling (MLM). At the *Subject Level* we similarly use ITC and ITM losses, but based on a single word noun. The motivation comes from the fact that a potentially much longer noun phrase, at the phrase level, may obfuscate text-image alignment by focusing more on adjectives (that maybe common among many phrases) as compared to the noun that tends to be more semantically important. The final, novel *Addition* loss, is formulated on emergent localization properties of VLMs [16, 24, 25] and requires the sum of the attention maps for the noun sub-phrases to be as close as possible to the combined composite phrase attention. This loss encourages the model to attend to multiple objects concurrently, rather than disproportionately focusing on the most prominent one. Collectively, these losses regularize training of VLMs, improving their performance, without requiring additional supervision beyond traditional image-caption pairs.

Contributions. Our contributions are two-fold:

- Based on syntactic parsing, we propose a Hierarchically STructured weakly-supervised framework (HIST) that improved image-text alignment in VLM training.
- We design two novel loss functions: (1) Subject Loss to ensure image alignment with both object-centric phrase and the subject, and (2) Addition Loss to encourage equal attention across multiple objects in a phrase.

Empirical results demonstrate the efficacy of our framework, showing an improvement of up to 9.8% on visual grounding and +6.3% on multi-object referring segmentation. Somewhat surprisingly, this approach, which was largely designed to improve *spatial* image-text alignment in VLMs, also benefits them more broadly with improvement of up to +1.1% on image-text retrieval, and +0.2% on visual question answering (VQA), underscoring the broader

¹We do this, instead of using the raw structure of the caption, in order to get richer syntactic structure potentially derived from multiple captions.

advantages of sentence structure modeling in VLMs.

2. Related Work

Vision-Language Models (VLMs). Vision-language pre-training (VLP) has established itself as a cornerstone in multimodal learning, driving advancements across tasks. Various architectures have been developed to optimize these tasks, including dual-encoders like CLIP [33] and ALIGN [15] for scalable contrastive learning, fusion-encoders like ALBEF [24] and LXMERT [38] for early cross-modal integration, and unified transformers such as BLIP [25] and BEiT [4], which consolidate multiple capabilities into a single model with both encoder and decoder architecture. Recently, VLMs have also begun integrating large language models (LLMs), as seen in BLIP2 [26] and LLaVA [29], enhancing multimodal interactions by combining powerful language understanding with visual components. Key training objectives in VLP have converged around image-text contrastive learning [23–25, 33, 37, 47], image-text matching [18, 23–25, 37, 43, 44, 47], and (masked) language modeling [2, 6, 23, 23, 25, 37, 44, 47], enabling refined and versatile multimodal understanding.

Despite these strides, most VLMs rely on pairwise image-text matching, often overlooking hierarchical structures in data, such as relationships among sub-phrases. Addressing this, our approach introduces hierarchical alignment, regularizing VLM learning with these nuanced relationships. This method enhances the model’s ability to localize and ground language-described entities in images; without the need for additional annotations or data.

Vision-Language Learning with Language Structure Supervised Losses. Several prior works have explored the benefits of leveraging language structure to enhance vision-language understanding. Early studies, such as [40], demonstrated the advantage of encoding textual hierarchical relationships (like generalization and entailment) in embedding spaces to improve tasks such as hypernym prediction, image-caption retrieval, and textual entailment. Another work [42] applied compositionality and exclusivity constraints, across noun phrases, to attention maps to improve visual grounding. However, these works were limited to smaller models and datasets, leaving open the question of to what extent these findings hold for the recent VLMs.

More recently, [8] introduces a semi-supervised approach that aligns image regions with corresponding noun phrases in captions, improving vision-language models (VLMs) on tasks such as visual question answering, visual commonsense reasoning, and visual grounding. Related, [5] examines how attributes, such as color, size, and texture, within image captions influence the learning and performance of vision-language models on open-vocabulary object detection and fine-grained text-region retrieval. SelfEQ [14] fine-tunes VLMs to produce consistent

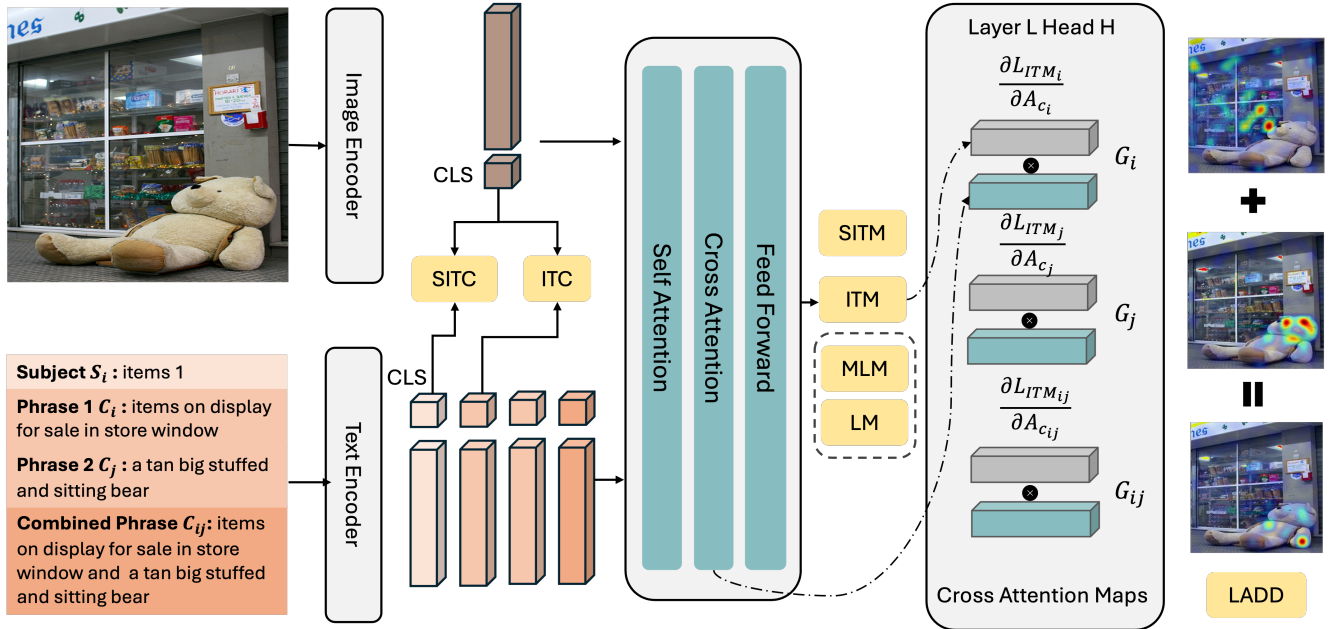


Figure 2. **The overall structure of HIST.** We decompose image captions into object-centric phrases and build a three-level hierarchy – *Subject* level, *Phrase* level, and *Composite Combined Phrase* level. Entailment between these constituent components of the sentence and the image, allows us to formulate additional regularization constraints for training of VLMs. Specifically, we leverage three losses. At the *Phrase* Level we ensure alignment (entailment) between noun phrases and the image by leveraging standard VLM losses typically applied for image-caption pairs: image-text contrastive (ITC), image-text matching (ITM), and masked language modeling (MLM) or language modeling (LM), depending on the model. At the *Subject* Level we similarly use ITC and ITM losses, but focus on matching the image and the subject noun of the phrase. This prevents adjectives in the phrase from obscuring the text-image alignment. The final *Addition* loss requires the sum of the attention maps for the noun phrases to be as close as possible to the combined composite phrase attention. This loss encourages the model to attend to multiple objects concurrently, rather than disproportionately focusing on the most prominent one.

visual explanations across paraphrased captions, showing marked improvements in visual grounding tasks.

Conceptually related [22] and [48] apply constraints to GradCAM maps according to linguistic structure, with the aim of enhancing visual grounding. In [48], dependency parsing on image captions is used to identify distinct objects and prevents overlapping attention maps between them, thereby improving model performance on visual grounding. [22] designs specific losses for referring segmentation, enforcing that words within the same noun phrase have similar GradCAM maps while suppressing attention on incorrect object regions based on relationships with neighboring words (building on observations in [42]).

We are inspired by [14] and [22], however, propose a formulation that models complementary sentence structure in terms of hierarchy of phrase and sub-phrase relations. As such, we posit that our losses and objectives can be combined with consistency [14] and exclusion [22] losses designed in those works. Moreover, we are the first, to our knowledge, to show that such regularization losses not only improve visual localization, but general VLM understanding.

3. Method

Our approach aims to improve the visual-textual alignment of VLMs by fine-tuning them with a novel Hierarchically Structured (HIST) set of losses for the constituent text phrases. Specifically, we decompose image captions into object-centric phrases and build a three-level hierarchy – *Subject* level, *Phrase* level, and *Composite Combined Phrase* level – as shown in Figure 1; with the steps specified in Algorithm 1 and Section 3.2. The hierarchical structure allows us to design training objectives that achieve more granular alignment between visual and textual features.

In Section 3.1, we first introduce preliminaries and the base model architectures to which we apply proposed HIST. These base models are typically optimized with three widely used losses formulated atop of image-text pairs: Image-Text Contrastive (ITC), Image-Text Matching (ITM), and Masked Language Modeling (MLM). We use these losses in conjunction with our hierarchically structured losses to fine-tune the base models. In Section 3.2, we present our hierarchical alignment objectives: the *Subject* loss and the *Addition* loss. The *Subject* loss aims to align the main subject of each noun phrase with its corresponding

Algorithm 1 Data Pair Creation: Noun Phrases Generation and Subject Constraints

Input: Dataset $\mathcal{D} = \{(\mathbf{I}_k, \text{cap}_{ik}) \mid k = 1, 2, \dots, M, i = 1, 2, \dots, N\}$, where each image \mathbf{I}_k has N captions, cap_{ik} , used to generate object-centric phrases.

Result: Set of data pairs \mathcal{P} .

```
1:  $\mathcal{P} \leftarrow \emptyset$  ▷ Initialize an empty set of pairs
2: for each  $(\mathbf{I}_k, \text{cap}_k)$  in  $\mathcal{D}$  do
3:    $\{(\mathbf{C}_1^k, S(\mathbf{C}_1^k)), \dots, (\mathbf{C}_N^k, S(\mathbf{C}_N^k))\} \leftarrow \text{LLM}(\text{cap}_k)$ 
   ▷ Generate noun phrases and their subject
4:   for each phrase  $\mathbf{C}_i^k$  in  $\{\mathbf{C}_1^k, \dots, \mathbf{C}_N^k\}$  do
5:     Candidates  $\leftarrow \{\mathbf{C}_j^k \mid j \neq i \wedge S(\mathbf{C}_j^k) \neq S(\mathbf{C}_i^k)\}$ 
6:     if Candidates  $\neq \emptyset$  then
7:       Randomly select  $\mathbf{C}_j^k$  from Candidates
8:        $\mathcal{P} \leftarrow \mathcal{P} \cup \{(\mathbf{I}_k, \mathbf{C}_i^k, \mathbf{C}_j^k)\}$ 
9:     end if
10:  end for
11: end for
12: return  $\mathcal{P}$ 
```

visual representation, enforcing consistency between subjects and corresponding phrases. The *Addition* loss further guides the model to attend to multiple objects within the same image by aggregating Grad-CAM maps across different phrases, ensuring that the model’s attention covers all relevant objects. This hierarchical loss structure allows our model to align fine-grained visual and textual details while maintaining global coherence across the image-text pair.

Experimentally, we show that these additional losses, that require no added supervision beyond image-text pairs, lead to significant improvement on grounding. Further, we show that they moderately improve performance on a variety of other downstream VLM tasks (see Sec. 4.3).

3.1. Base Model and Objectives

Our formulation, HIST, is applicable to any VLM model that is capable of obtaining spatial image-text attention. We illustrate its efficacy on two popular VLM models: ALBEF [24] and BLIP [25]. Both of these models consist of an unimodal image encoder ϕ_v , a unimodal text encoder ϕ_t , and a multimodal encoder ϕ_m . The output of the image encoder and text encoder are represented as $\mathbf{V} = \{\mathbf{v}_{cls}, \mathbf{v}_1, \dots, \mathbf{v}_{N_v}\} \in \mathbb{R}^{(N_v+1) \times d_v}$, where N_v is the number of visual tokens and d_v is the visual embedding dimension, and $\mathbf{T} = \{\mathbf{t}_{cls}, \mathbf{t}_1, \dots, \mathbf{t}_{N_t}\} \in \mathbb{R}^{(N_t+1) \times d_t}$ where N_t is the number of text tokens and d_t is the text embedding dimension. Both models utilize the three commonly used objectives for learning visual and textual representations: image-text contrastive (ITC), image-text matching (ITM), masked language modeling (MLM). We provide a brief overview of these objectives here as we also leverage them during our training.

Image-Text Contrastive Learning (ITC). The ITC objective aims to align unimodal representations by maximizing similarity for matching image-text pairs and minimizing it for non-matching pairs. For an image \mathbf{I} and text \mathbf{T} , we define the similarity as:

$$s(\mathbf{I}, \mathbf{T}) = g_v(\mathbf{v}_{cls})^\top g_t(\mathbf{t}_{cls}),$$

where g_v and g_t are linear projections of the [CLS] token from the image patches embedding and the text embedding.

The image-to-text and text-to-image similarities are calculated as:

$$p_m^{i2t}(\mathbf{I}) = \frac{\exp(s(\mathbf{I}, \mathbf{T}_m)/\tau)}{\sum_{m=1}^M \exp(s(\mathbf{I}, \mathbf{T}_m)/\tau)},$$
$$p_m^{t2i}(\mathbf{T}) = \frac{\exp(s(\mathbf{T}, \mathbf{I}_m)/\tau)}{\sum_{m=1}^M \exp(s(\mathbf{T}, \mathbf{I}_m)/\tau)},$$

where τ is a temperature parameter and M being the image or text queue following MoCo [13]. The ITC loss is defined as follows:

$$\mathcal{L}_{\text{itc}} = \frac{1}{2} \mathbb{E}_{(\mathbf{I}, \mathbf{T}) \sim \mathcal{D}} \left[\mathcal{H}(y^{i2t}(\mathbf{I}), p^{i2t}(\mathbf{I})) + \mathcal{H}(y^{t2i}(\mathbf{T}), p^{t2i}(\mathbf{T})) \right],$$

where $y^{i2t}(\mathbf{I})$ and $y^{t2i}(\mathbf{T})$ are one-hot ground-truth vectors, \mathcal{H} denotes the cross-entropy, and \mathbb{E} is expectation over the training dataset \mathcal{D} in image-text pairs.

Image-Text Matching (ITM). The ITM objective predicts whether an image-text pair (\mathbf{I}, \mathbf{T}) is positive (matched) or negative (not matched). This is achieved by passing the fused [CLS] embedding from the multimodal encoder through a fully connected layer followed by a softmax to predict a binary probability $p^{\text{itm}}(\mathbf{I}, \mathbf{T})$. The ITM loss \mathcal{L}_{itm} is defined as:

$$\mathcal{L}_{\text{itm}} = \mathbb{E}_{(\mathbf{I}, \mathbf{T}) \sim \mathcal{D}} \mathcal{H}(y^{\text{itm}}, p^{\text{itm}}(\mathbf{I}, \mathbf{T})),$$

where y^{itm} is a two-dimensional one-hot vector representing the ground-truth label (matched or not).

Masked Language Modeling (MLM). Masked Language Modeling (MLM) integrates contextual information from both the text and the paired image to predict masked tokens within the text. Tokens in the input text are randomly masked out and replaced with a special [MASK] token. Let $\hat{\mathbf{T}}$ denote the masked text and $p^{\text{msk}}(\mathbf{I}, \hat{\mathbf{T}})$ denote the model’s predicted probability distribution for the masked token. The MLM objective \mathcal{L}_{mlm} minimizes the cross-entropy loss:

$$\mathcal{L}_{\text{mlm}} = \mathbb{E}_{(\mathbf{I}, \hat{\mathbf{T}}) \sim \mathcal{D}} \mathcal{H}(y^{\text{msk}}, p^{\text{msk}}(\mathbf{I}, \hat{\mathbf{T}})),$$

where y^{msk} is a one-hot distribution representing the ground-truth token for the masked position.

Certain VLMs though, like BLIP [25], use a language modeling loss focused on predicting the next word token rather than randomly masking words within sentences and predicting the masked tokens. Essentially, this approach uses a cross-entropy loss for next-word prediction.

3.2. Hierarchically Structured (HIST) Losses

To enhance cross-modal alignment at different levels of granularity, we introduce two additional sets of hierarchically structured losses which we describe in this section; mainly the *Subject* and the *Addition* loss.

Phrase parsing. As illustrated in Algorithm 1, we follow SelfEQ [14] and perform phrase chunking using Vicuna [7]. Specifically, in-context examples are provided to Vicuna [7] to first generate noun phrases from caption, and then each noun phrase is re-inputted to Vicuna to detect the subject. To construct composite phrase dataset \mathcal{P} , for each noun phrase \mathbf{C}_i^k , we identify potential pairing candidates $\{\mathbf{C}_j^k\}$ from other noun phrases from the same image but not referring to the same subject (these do not necessarily come from the same caption). We then randomly select a pairing candidate and form a data pair $(\mathbf{I}_k, \mathbf{C}_i^k, \mathbf{C}_j^k)$, and add it to \mathcal{P} . This process repeats for all phrases in each caption, ultimately generating \mathcal{P} , which contains the selected image-composite caption phrase pairs for further use.

Phrase Loss. With the noun phrases we obtained above, we apply the ITC, ITM and MLM on the phrases directly: $\mathcal{L}_{phrase} =$

$$\mathcal{L}_{ITC}(\{(\mathbf{I}, \mathbf{C}_i)\}) + \mathcal{L}_{ITM}(\{(\mathbf{I}, \mathbf{C}_i)\}) + \mathcal{L}_{MLM}(\{(\mathbf{C}_i)\}).$$

Subject Loss. The motivation of the *Subject* loss comes from the fact that a potentially much longer noun phrase, at the phrase level, may obfuscate text-image alignment by focusing more on adjectives (that maybe common among many phrases) as compared to the noun that tends to be more semantically important. With such an observation, we add a *Subject* Loss during training, which enforces consistency, aligning the subject of the phrase with the corresponding visual representation. Specifically, for a phrase \mathbf{C}_i with main subject \mathbf{S}_i , the loss is:

$$\mathcal{L}_{subject} = \mathcal{L}_{ITC}(\{(\mathbf{I}, \mathbf{S}_i)\}) + \mathcal{L}_{ITM}(\{(\mathbf{I}, \mathbf{S}_i)\}).$$

where \mathcal{L}_{ITC} and \mathcal{L}_{ITM} are defined above.

Localization in VLMs. We first introduce how we obtain localization map for phrases and then discuss the novel *Addition* loss we proposed.

The text prompt and the image first go through the modality-specific encoders ϕ_t and ϕ_v respectively, then the respective embeddings are input into the cross-attention fusion module. For each cross-attention layer, the text en-

codings serve as query vectors and the image patch encodings are as key and value vectors. From a particular cross-attention layer (and specific head), we extract the corresponding text-to-image cross-attention map as shown below. Note that different layers and heads lead to drastic performance differences, and we follow [14, 16] for the best layer-head combination; resulting in

$$\mathbf{A}_{\mathbf{C}_i} = \text{Softmax} \left(\frac{\phi_t(\mathbf{T}) \mathbf{W}_Q (\phi_v(\mathbf{I}) \mathbf{W}_K)^\top}{\sqrt{D_t}} \right),$$

where $\mathbf{A}_{\mathbf{C}_i}$ has shape $(K + 1) \times P \times P$ with P being the number of image patches and K being the number of text tokens. To get the phrase specific attention map, we take the mean over all K tokens and get final map of size $P \times P$. This map can serve as proxy for segmentation [16] and can further be enhanced by GradCAM [34], to highlight discriminative regions, as shown in [16, 39]. Applying this technique results in the final localization map:

$$\mathbf{G}_{\mathbf{C}_i} = \text{ReLU} \left(\mathbf{A}_{\mathbf{C}_i} \cdot \frac{\partial \mathcal{L}_{ITM,i}}{\partial \mathbf{A}_{\mathbf{C}_i}} \right),$$

for a given phrase \mathbf{C}_i and a particularly chosen attention layer and head. This final localization map is obtained by taking the element-wise product of the cross-attention map with a gradient of the loss $\mathcal{L}_{ITM,i}$ with respect to it.

Addition Loss. We are now ready to define our novel *Addition* loss at the combined phrase level. For a pair of phrases $\mathbf{C}_i, \mathbf{C}_j$, extracted from captions of the same image, and the combined composite phrase \mathbf{C}_{ij} we extract the cross-attention maps and then the corresponding localization maps as follows:

$$\begin{aligned} \mathbf{G}_{\mathbf{C}_i} &= \text{ReLU} \left(\mathbf{A}_{\mathbf{C}_i} \cdot \frac{\partial \mathcal{L}_{ITM,i}}{\partial \mathbf{A}_{\mathbf{C}_i}} \right), \\ \mathbf{G}_{\mathbf{C}_j} &= \text{ReLU} \left(\mathbf{A}_{\mathbf{C}_j} \cdot \frac{\partial \mathcal{L}_{ITM,j}}{\partial \mathbf{A}_{\mathbf{C}_j}} \right), \\ \mathbf{G}_{\mathbf{C}_{ij}} &= \text{ReLU} \left(\mathbf{A}_{\mathbf{C}_{ij}} \cdot \frac{\partial \mathcal{L}_{ITM,ij}}{\partial \mathbf{A}_{\mathbf{C}_{ij}}} \right). \end{aligned}$$

We observed that vision-language models often focus disproportionately on the most prominent objects within an image, which can lead to poor alignment. Therefore, we introduce the *Addition* loss to improve the model’s capacity to attend to multiple objects simultaneously. It is defined as:

$$\mathcal{L}_{add} = \sum_P \sum_P |\mathbf{G}_{\mathbf{C}_i} + \mathbf{G}_{\mathbf{C}_j} - \mathbf{G}_{\mathbf{C}_{ij}}|.$$

The loss enforces that the attention map for the combined phrase approximates the sum of individual attention maps, ensuring that the model considers all relevant objects.

3.3. Total Hierarchical Alignment Loss

The total loss combines all the losses mentioned above:

$$\mathcal{L}_{\text{total}} = \mathcal{L}_{\text{phrase}} + \mathcal{L}_{\text{subject}} + \mathcal{L}_{\text{add}}.$$

This hierarchical loss formulation allows our model to align fine-grained visual and textual semantics effectively, while maintaining global coherence across the image-text pair. Each component contributes to a specific level of alignment, from individual phrases to subjects and combined phrases, ultimately refining the model’s ability to handle complex, multi-object scenes and improving its localization ability.

4. Experiment

Implementation details. We apply HIST on ALBEF [24] and BLIP [25] and train the model with Visual Genome [21] and MSCOCO [28]. ALBEF combines a ViT-B model for encoding images and a BERT_{base} model for encoding text. Following SelfEQ [14], we train ALBEF with image size of 256×256 with the composite objective function $\mathcal{L} = \alpha \mathcal{L}_{\text{vi}} + (1 - \alpha) (\mathcal{L}_{\text{vi}} + \mathcal{L}_{\text{HIST}})$, where α is initially set to 0 and increments to 1, remaining constant after the second epoch. We train our model with with 4 NVIDIA A6000 with learning rate of $2e-5$. For the addition loss, we employ the head average gradcam map from the 3rd cross-attention layer. For BLIP, we train BLIP_{large}, which adopts ViT-L/16 as the image encoder, BERT as the text encoder, and insert an extra cross-attention layer for each transformer block of BERT. Following BLIP [25], we train BLIP with image size of 224×224 , on 4 NVIDIA A6000 with learning rate $1e-5$. For the addition loss, we leverage the head average gradcam map from the 9th cross-attention layer. [We will release all models, data and code upon acceptance of the paper.](#)

4.1. Visual Grounding

We evaluate ALBEF [24] and BLIP [25] on the test splits of Flickr30k [31] and ReferIt [17], which contain 1k and 10k images, respectively, following [1, 14]. Additionally, following SelfEQ [14], we assess our method on RefCOCO+ [46] Test A and Test B, a challenging benchmark for box-supervised methods. We use pointing game accuracy [49] for evaluation. It measures the percentage of test pairs where the highest point in the predicted heatmap for each pair falls within the ground-truth bounding box.

As observed in Table 1, when applying HIST to the base model ALBEF, we achieve an absolute performance gain of 4.2% on Flickr30K and 9.8% on ReferIt when trained with Visual Genome [21], and gains of 5.9% on Flickr30K and 3.7% on ReferIt when trained with MSCOCO [28]. Similarly, applying HIST to the base model BLIP yields a performance improvement of 1.4% on Flickr30K and 6.5% on ReferIt with Visual Genome [21], and improvement of 4.6% on Flickr30K and 6.0% on ReferIt with MSCOCO [28].

Method	Training	Flickr30K	Referit
InfoGround [12]	VG-boxes	76.7	-
VMRM [9]	VG-boxes	81.1	-
AMC [45]	VG-boxes	86.6	73.2
ALBEF [24]	Zero-shot	79.4	59.7
BLIP [25]	Zero-shot	80.1	51.6
g [36]	VG	75.6	66.0
g++ [35]	VG	80.0	70.3
ALBEF + SelfEQ [14]	VG	81.9	67.4
(Ours) ALBEF + HIST	VG	83.6	69.5
(Ours) BLIP + HIST	VG	81.5	58.1
g [36]	COCO	75.4	61.0
g++ [35]	COCO	78.1	61.5
ALBEF + SelfEQ [14]	COCO	84.1	62.8
(Ours) ALBEF + HIST	COCO	85.3	63.4
(Ours) BLIP + HIST	COCO	84.7	57.6

Table 1. **Visual Grounding on Flickr30K [31] and Referit [17].** VG stands for Visual Genome. Our HIST atop of ALBEF and BLIP outperform baselines and SelfEQ [14] variants.

Method	Training	RefCOCO+	
		Test A	Test B
InfoGround [12]	VG-boxes	39.8	44.1
VMRM [9]	VG-boxes	58.9	50.3
AMC [45]	VG-boxes	80.3	64.6
ALBEF [24]	Zero-shot	69.4	53.8
BLIP [25]	Zero-shot	70.2	52.4
ALBEF + SelfEQ [†] [14]	VG	74.1	55.1
ALBEF + SelfEQ [14]	VG	75.1	55.5
(Ours) ALBEF + HIST	VG	74.7	56.7
(Ours) BLIP + HIST	VG	75.3	56.4

Table 2. **Visual Grounding on RefCOCO+ [46].** VG stands for Visual Genome. [†] represent our rerun result.

Notably, we also outperform the state-of-the-art in Visual Grounding. Compared to the recent approach SelfEQ [14], which uses the same backbone and training data, we achieve an improvement of 1.7% on Flickr30k and 2.1% on ReferIt when trained on Visual Genome, and 1.2% on Flickr30k and 0.6% on ReferIt when trained on MSCOCO. Our method also performs comparably to methods using bounding box supervision on Flickr30k. Although our performance for visual grounding on Referit is marginally lower than g++ [35], it is worth noting that their approach benefits from additional supervision through the use of heatmaps from CLIP as pseudo-labels; Our method can potentially benefit from similar supervision.

Following SelfEQ [14], we also evaluate our method

Method	Training	CIoU
ALBEF [24]	Zero-shot	29.4
ALBEF + SelfEQ [14]	COCO	30.3
(Ours) ALBEF + HIST	COCO	35.6

Table 3. **Complex Referring Segmentation on RefCOCO+ [46].**

(trained with VG) on RefCOCO+ [46], a more rigorous benchmark, typically used to assess box-supervised techniques, with 750 images in each of the Test A and Test B sets. As shown in Table 2, we outperform the base model ALBEF by 5.3% and 2.9% on Test A and Test B respectively. Additionally, we achieve a 0.6% improvement on RefCOCO+ Test A and a 1.6% improvement on RefCOCO+ Test B compared to SelfEQ. Applying HIST with BLIP, we obtain a substantial improvement of 5.3% / 4.4% on RefCOCO+ Test A / Test B over zero-shot evaluation.

We could not directly compare with CAFT [48] as we were unable to replicate the baseline performance reported in their work². However, our improvements over the ALBEF baseline are relatively larger compared to CAFT. Notably, our losses and objectives are different and complementary to both SelfEQ [14] and CAFT [48], allowing our method to be integrated with their losses for potential gains.

4.2. Complex Referring Segmentation

For Referring Segmentation, we focus on the RefCOCO+ [46] dataset to evaluate HIST’s performance in multi-object scenarios. We developed a custom multi-object referring segmentation test set from RefCOCO+ [46]. For each image in the RefCOCO+ test set that contains two or more text phrases, we randomly select two phrases and combine them using an “and”. This yields 1,404 unique image-text pairs designed to assess the ability to handle complex multi-object references.

To isolate the model’s localization ability from segmentation mask completeness, we utilize SAM [19] as a post-processing tool. For each method, we first get the location of the top 4 patches in the $P \times P$ predicted heatmap, then we scale it to the corresponding location in the original image dimension. These points serve as the input to SAM to obtain corresponding object masks. We report CIoU following standard referring segmentation evaluation metrics [50, 51].

As shown in Table 3, we outperform both ALBEF and SelfEQ [14] by 6.2% and 5.3%, respectively, on the complex scene referring segmentation. Additionally, Figure 3 shows qualitative comparisons among ALBEF, ALBEF + SelfEQ, and ALBEF + HIST. We observe that ALBEF + HIST significantly outperforms ALBEF and ALBEF + SelfEQ in indentifying complex queries involving multiple

²ALBEF’s performance on Flickr30K is reported as 84.49 in [48], while SelfEQ [14] and our experiments find it to be 79.4.

objects within intricate scenes. For instance, it accurately identifies the “Blurry pie” in a blurry image, the occluded “Not full zebra” and relative object positions such as “The further meter,” the “Nearest meter,” and the “Lady in the back.” This enhanced ability to distinguish multiple objects in challenging contexts underscores HIST’s robustness and effectiveness in visual grounding tasks. (More qualitative result provided in the supplementary.)

4.3. Downstream Tasks

While our losses were designed to improve localization, we also test the impact of they have on other downstream VLM tasks, including image-text retrieval and VQA.

Image-Text Retrieval. For Image-Text Retrieval, we use the MSCOCO [28] and Flickr30k [31] datasets. We evaluate ALBEF + HIST (trained with VG) for both image-to-text retrieval (TR) and text-to-image retrieval (IR). Following ALBEF [24], we finetune the pre-trained model using ITC and ITM losses and the training samples from the respective datasets. We report average recall@1 for this task. From Table 4, we observe that compared to ALBEF, ALBEF + HIST gives 1.1% improvement on image-to-text retrieval recall@1 and 0.7% on text-to-image retrieval recall@1 when finetune on COCO, and 0.2% improvement on image-to-text retrieval recall@1 and 0.4% on text-to-image retrieval recall@1 when finetune on Flickr30k.

Method	Retrieval-FT COCO		Retrieval-FT Flickr30k	
	TR@1	IR@1	TR@1	IR@1
ALBEF [24]	77.6	60.7	95.9	85.6
(Ours) ALBEF + HIST	78.7	61.4	96.1	86.0

Table 4. **Image-Text Retrieval on COCO [28] and Flickr30K [31].** We train ALBEF with HIST on Visual Genome.

Visual Question Answering. For VQA, we use the VQA [11] dataset. Following ALBEF, we fine-tune a 6-layer transformer decoder to generate answers, initializing it with pre-trained weights from the multimodal encoder of HIST + ALBEF. As shown in Table 5, We observe +0.2% improvement on VQA-dev and VQA-std.

Method	VQA-dev	VQA-std
ALBEF [24]	75.8	76.0
(Ours) ALBEF + HIST	76.0	76.2

Table 5. **Visual Question Answering on VQA [11].** We train ALBEF with HIST on Visual Genome.

4.4. Ablation Study

HIST Losses. We ablate different loss components of HIST + ALBEF and report the results in Tab. 6. Each component

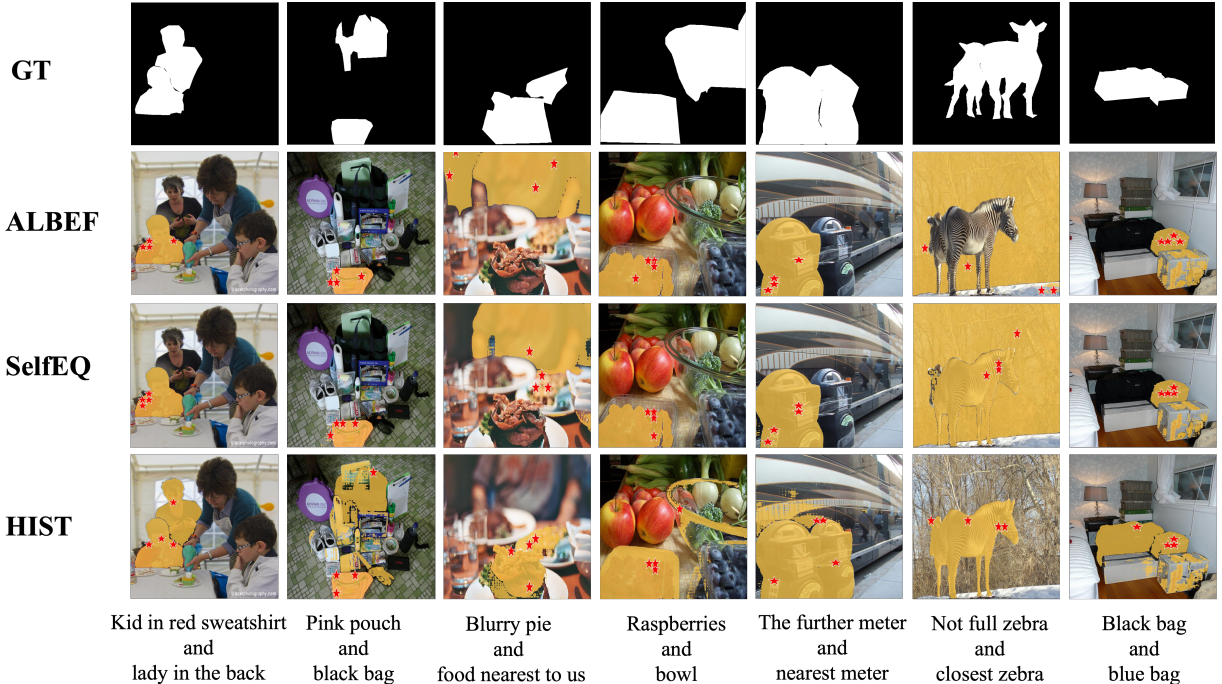


Figure 3. **Qualitative Result for ALBEF, SelfEQ and HIST + ALBEF on Visual Grounding and Referring Segmentation.** Images are from RefCOCO+. The enlarged red stars represent the top 4 locations with the highest predicted attention value from respective methods. To obtain segmentation mask, we input the four points into SAM [19] as point prompts. We note that the HIST accurately detect all objects but the mask can over-segment or under-segment.

contributes positively to the final performance, which highlights the significance of our design choices.

Data	Objective	Flickr30k
-	\mathcal{L}_{vl}	79.4
T	\mathcal{L}_{phrase}	81.6
T_{HIST}	$\mathcal{L}_{phrase} + \mathcal{L}_{add}$	85.0
T_{HIST}	$\mathcal{L}_{phrase} + \mathcal{L}_{subj} + \mathcal{L}_{add}$	85.3

Table 6. **Ablation on HIST Losses.** Models are trained with COCO. T represents training with only noun phrases of COCO. T_{HIST} represents training with our HIST structure.

BLIP Layer and Head effect. As shown in Table 7, our experiments demonstrate that when training BLIP with HIST, using the head average attention map from the 9th cross-attention layer to calculate the *Addition* Loss enhances grounding performance in both layer 9 head 10, and layer 8 head 10 of BLIP. Consequently, we report BLIP’s visual grounding performance by training with the *Addition* loss using the head average Grad-CAM map from the 9th cross-attention layer and evaluate using the mean of two attention maps: (1) layer 9 head 10 and (2) layer 8 head 10.

Train Eval	L8	L9	L8H10	L9H10	Mean	Mul
	L8H10	51.1	56.9	42.9	56.5	48.9
L9H10	48.3	51.8	53.9	32.4	17.1	32.4
Mean	51.2	57.6	53.9	56.7	18.7	56.8
Mul	52.4	56.2	53.7	49.6	21.4	49.6

Table 7. **Ablation of HIST + BLIP on layer and head.** We train HIST+BLIP on COCO and test on Referit with image size of 384. Mean represent the average of attention maps from L8H10 and L9H10 of BLIP. Mul represent the element-wise multiplication of attention maps from L8H10 and L9H10 of BLIP.

5. Conclusion

We present a novel Hierarchically Structured (HIST) learning framework that enhances vision-language alignment in Vision-Language Models (VLMs) by embedding hierarchical syntactic structures into training. HIST organizes captions into structured noun phrases across multiple syntactic levels, improving alignment at both phrase and object levels without additional supervision. Our framework introduces two key losses: *Subject Loss*, ensuring alignment with object-centric phrases and subjects, and *Addition Loss*, promoting balanced attention across multiple objects in complex scenes. HIST significantly enhances localization in

challenging multi-object scenes and improves performance in tasks like image-text retrieval and visual question answering, underscoring the value of hierarchical structuring for spatial and semantic alignment in VLMs.

References

- [1] Hassan Akbari, Svebor Karaman, Surabhi Bhargava, Brian Chen, Carl Vondrick, and Shih-Fu Chang. Multi-level multi-modal common semantic space for image-phrase grounding. In *IEEE Conf. Comput. Vis. Pattern Recog.*, pages 12476–12486, 2019. 6
- [2] Jean-Baptiste Alayrac, Jeff Donahue, Pauline Luc, Antoine Miech, Iain Barr, Yana Hasson, Karel Lenc, Arthur Mensch, Katherine Millican, Malcolm Reynolds, Roman Ring, Eliza Rutherford, Serkan Cabi, Tengda Han, Zhitao Gong, Sina Samangooei, Marianne Monteiro, Jacob L Menick, Sebastian Borgeaud, Andy Brock, Aida Nematzadeh, Sahand Sharifzadeh, Mikolaj Bińkowski, Ricardo Barreira, Oriol Vinyals, Andrew Zisserman, and Karén Simonyan. Flamingo: a visual language model for few-shot learning. In *Adv. Neural Inform. Process. Syst.*, 2022. 1, 2
- [3] Jacob Andreas, Andreas Vlachos, and Stephen Clark. Semantic parsing as machine translation. In *Proceedings of the 51st Annual Meeting of the Association for Computational Linguistics (Volume 2: Short Papers)*, pages 47–52, 2013. 1
- [4] Hangbo Bao, Li Dong, Songhao Piao, and Furu Wei. Beit: Bert pre-training of image transformers. *arXiv preprint arXiv:2106.08254*, 2021. 2
- [5] Kyle Buettner and Adriana Kovashka. Investigating the role of attribute context in vision-language models for object recognition and detection. In *Proceedings of the IEEE/CVF Winter Conference on Applications of Computer Vision*, pages 5474–5484, 2024. 2
- [6] Jun Chen, Han Guo, Kai Yi, Boyang Li, and Mohamed Elhoseiny. Visualgpt: Data-efficient adaptation of pretrained language models for image captioning. In *IEEE Conf. Comput. Vis. Pattern Recog.*, pages 18030–18040, 2022. 2
- [7] Wei-Lin Chiang, Zhuohan Li, Zi Lin, Ying Sheng, Zhanghao Wu, Hao Zhang, Lianmin Zheng, Siyuan Zhuang, Yonghao Zhuang, Joseph E Gonzalez, et al. Vicuna: An open-source chatbot impressing gpt-4 with 90%* chatgpt quality. See <https://vicuna.lmsys.org> (accessed 14 April 2023), 2(3):6, 2023. 5
- [8] Shih-Han Chou, Zicong Fan, James J Little, and Leonid Sigal. Semi-supervised grounding alignment for multi-modal feature learning. In *2022 19th Conference on Robots and Vision (CRV)*, pages 48–57. IEEE, 2022. 2
- [9] Zi-Yi Dou and Nanyun Peng. Improving pre-trained vision-and-language embeddings for phrase grounding. In *Proceedings of the 2021 Conference on Empirical Methods in Natural Language Processing*, pages 6362–6371, 2021. 6
- [10] Akiko Eriguchi, Yoshimasa Tsuruoka, and Kyunghyun Cho. Learning to parse and translate improves neural machine translation. *arXiv preprint arXiv:1702.03525*, 2017. 1
- [11] Yash Goyal, Tejas Khot, Douglas Summers-Stay, Dhruv Batra, and Devi Parikh. Making the v in vqa matter: Elevating the role of image understanding in visual question answering. In *IEEE Conf. Comput. Vis. Pattern Recog.*, pages 6904–6913, 2017. 1, 7
- [12] Tanmay Gupta, Arash Vahdat, Gal Chechik, Xiaodong Yang, Jan Kautz, and Derek Hoiem. Contrastive learning for weakly supervised phrase grounding. In *Eur. Conf. Comput. Vis.*, pages 752–768. Springer, 2020. 6
- [13] Kaiming He, Haoqi Fan, Yuxin Wu, Saining Xie, and Ross Girshick. Momentum contrast for unsupervised visual representation learning. In *IEEE Conf. Comput. Vis. Pattern Recog.*, pages 9729–9738, 2020. 4
- [14] Ruozhen He, Paola Cascante-Bonilla, Ziyang Yang, Alexander C Berg, and Vicente Ordonez. Improved visual grounding through self-consistent explanations. In *IEEE Conf. Comput. Vis. Pattern Recog.*, pages 13095–13105, 2024. 2, 3, 5, 6, 7
- [15] Chao Jia, Yinfei Yang, Ye Xia, Yi-Ting Chen, Zarana Parekh, Hieu Pham, Quoc Le, Yun-Hsuan Sung, Zhen Li, and Tom Duerig. Scaling up visual and vision-language representation learning with noisy text supervision. In *Int. Conf. Machine Learning*, 2021. 1, 2
- [16] Luo Jiayun, Siddhesh Khandelwal, Leonid Sigal, and Boyang Li. Plug-and-play, dense-label-free extraction of open-vocabulary semantic segmentation from vision-language models. *IEEE Conf. Comput. Vis. Pattern Recog.*, 2024. 2, 5
- [17] Sahar Kazemzadeh, Vicente Ordonez, Mark Matten, and Tamara Berg. Referitgame: Referring to objects in photographs of natural scenes. In *Proceedings of the 2014 conference on empirical methods in natural language processing (EMNLP)*, pages 787–798, 2014. 1, 6
- [18] Wonjae Kim, Bokyung Son, and Ildoo Kim. Vilt: Vision-and-language transformer without convolution or region supervision. In *Int. Conf. Machine Learning*, 2021. 1, 2
- [19] Alexander Kirillov, Eric Mintun, Nikhila Ravi, Hanzi Mao, Chloe Rolland, Laura Gustafson, Tete Xiao, Spencer Whitehead, Alexander C Berg, Wan-Yen Lo, et al. Segment anything. In *Proceedings of the IEEE/CVF International Conference on Computer Vision*, pages 4015–4026, 2023. 7, 8
- [20] Alexandros Komninos and Suresh Manandhar. Dependency based embeddings for sentence classification tasks. In *Proceedings of the 2016 conference of the North American chapter of the association for computational linguistics: human language technologies*, pages 1490–1500, 2016. 1
- [21] Ranjay Krishna, Yuke Zhu, Oliver Groth, Justin Johnson, Kenji Hata, Joshua Kravitz, Stephanie Chen, Yannis Kalantidis, Li-Jia Li, David A Shamma, et al. Visual genome: Connecting language and vision using crowdsourced dense image annotations. *International journal of computer vision*, 123:32–73, 2017. 6
- [22] Jungbeom Lee, Sungjin Lee, Jinseok Nam, Seunghak Yu, Jaeyoung Do, and Tara Taghavi. Weakly supervised referring image segmentation with intra-chunk and inter-chunk consistency. In *Int. Conf. Comput. Vis.*, pages 21870–21881, 2023. 3
- [23] Chenliang Li, Haiyang Xu, Junfeng Tian, Wei Wang, Ming Yan, Bin Bi, Jiabo Ye, Hehong Chen, Guohai Xu, Zheng

- Cao, et al. mplug: Effective and efficient vision-language learning by cross-modal skip-connections. *arXiv preprint arXiv:2205.12005*, 2022. 1, 2
- [24] Junnan Li, Ramprasaath R. Selvaraju, Akhilesh Deepak Gotmare, Shafiq Joty, Caiming Xiong, and Steven Hoi. Align before fuse: Vision and language representation learning with momentum distillation. In *Adv. Neural Inform. Process. Syst.*, 2021. 2, 4, 6, 7
- [25] Junnan Li, Dongxu Li, Caiming Xiong, and Steven Hoi. Blip: Bootstrapping language-image pre-training for unified vision-language understanding and generation. In *Int. Conf. Machine Learning*, pages 12888–12900. PMLR, 2022. 1, 2, 4, 5, 6
- [26] Junnan Li, Dongxu Li, Silvio Savarese, and Steven Hoi. Blip-2: Bootstrapping language-image pre-training with frozen image encoders and large language models. In *Int. Conf. Machine Learning*, 2023. 2
- [27] Xiujun Li, Xi Yin, Chunyuan Li, Pengchuan Zhang, Xiaowei Hu, Lei Zhang, Lijuan Wang, Houdong Hu, Li Dong, Furu Wei, Yejin Choi, and Jianfeng Gao. Oscar: Object-semantics aligned pre-training for vision-language tasks. In *Eur. Conf. Comput. Vis.*, 2020. 1
- [28] Tsung-Yi Lin, Michael Maire, Serge Belongie, James Hays, Pietro Perona, Deva Ramanan, Piotr Dollár, and C. Lawrence Zitnick. Microsoft coco: Common objects in context. In *Eur. Conf. Comput. Vis.*, pages 740–755, 2014. 1, 6, 7
- [29] Haotian Liu, Chunyuan Li, Qingyang Wu, and Yong Jae Lee. Visual instruction tuning. In *Adv. Neural Inform. Process. Syst.*, 2023. 1, 2
- [30] Martin J Pickering and Roger PG Van Gompel. Syntactic parsing. In *Handbook of psycholinguistics*, pages 455–503. Elsevier, 2006. 1
- [31] Bryan A Plummer, Liwei Wang, Chris M Cervantes, Juan C Caicedo, Julia Hockenmaier, and Svetlana Lazebnik. Flickr30k entities: Collecting region-to-phrase correspondences for richer image-to-sentence models. In *Int. Conf. Comput. Vis.*, pages 2641–2649, 2015. 1, 6, 7
- [32] Vasin Punyakanok, Dan Roth, and Wen-tau Yih. The importance of syntactic parsing and inference in semantic role labeling. *Computational Linguistics*, 34(2):257–287, 2008. 1
- [33] Alec Radford, Jong Wook Kim, Chris Hallacy, Aditya Ramesh, Gabriel Goh, Sandhini Agarwal, Girish Sastry, Amanda Askell, Pamela Mishkin, Jack Clark, Gretchen Krueger, and Ilya Sutskever. Learning transferable visual models from natural language supervision. In *Int. Conf. Machine Learning*, 2021. 1, 2
- [34] Ramprasaath R. Selvaraju, Michael Cogswell, Abhishek Das, Ramakrishna Vedantam, Devi Parikh, and Dhruv Batra. Grad-cam: Visual explanations from deep networks via gradient-based localization. In *Int. Conf. Comput. Vis.*, 2017. 5
- [35] Tal Shaharabany and Lior Wolf. Similarity maps for self-training weakly-supervised phrase grounding. In *IEEE Conf. Comput. Vis. Pattern Recog.*, pages 6925–6934, 2023. 6
- [36] Tal Shaharabany, Yoad Tewel, and Lior Wolf. What is where by looking: Weakly-supervised open-world phrase-grounding without text inputs. *Adv. Neural Inform. Process. Syst.*, 35:28222–28237, 2022. 6
- [37] Amanpreet Singh, Ronghang Hu, Vedanuj Goswami, Guillaume Couairon, Wojciech Galuba, Marcus Rohrbach, and Douwe Kiela. Flava: A foundational language and vision alignment model. In *IEEE Conf. Comput. Vis. Pattern Recog.*, pages 15638–15650, 2022. 1, 2
- [38] Hao Tan and Mohit Bansal. Lxmert: Learning cross-modality encoder representations from transformers. *arXiv preprint arXiv:1908.07490*, 2019. 2
- [39] Anthony Meng Huat Tiong, Junnan Li, Boyang Li, Silvio Savarese, and Steven CH Hoi. Plug-and-play vqa: Zero-shot vqa by conjoining large pretrained models with zero training. *arXiv preprint arXiv:2210.08773*, 2022. 5
- [40] Ivan Vendrov, Ryan Kiros, Sanja Fidler, and Raquel Urtasun. Order-embeddings of images and language. *arXiv preprint arXiv:1511.06361*, 2015. 1, 2
- [41] Yongliang Wu, Shuliang Zhao, and Wenbin Li. Phrase2vec: phrase embedding based on parsing. *Information Sciences*, 517:100–127, 2020. 1
- [42] Fanyi Xiao, Leonid Sigal, and Yong Jae Lee. Weakly-supervised visual grounding of phrases with linguistic structures. In *IEEE Conf. Comput. Vis. Pattern Recog.*, pages 5945–5954, 2017. 1, 2, 3
- [43] Haiyang Xu, Qinghao Ye, Ming Yan, Yaya Shi, Jiabo Ye, Yuanhong Xu, Chenliang Li, Bin Bi, Qi Qian, Wei Wang, et al. mplug-2: A modularized multi-modal foundation model across text, image and video. In *Int. Conf. Machine Learning*, pages 38728–38748. PMLR, 2023. 2
- [44] Xiao Xu, Chenfei Wu, Shachar Rosenman, Vasudev Lal, Wanxiang Che, and Nan Duan. Bridgetower: Building bridges between encoders in vision-language representation learning. In *AAAI*, pages 10637–10647, 2023. 1, 2
- [45] Ziyang Yang, Kushal Kafle, Franck Dernoncourt, and Vicente Ordonez. Improving visual grounding by encouraging consistent gradient-based explanations. In *IEEE Conf. Comput. Vis. Pattern Recog.*, pages 19165–19174, 2023. 6
- [46] Licheng Yu, Patrick Poirson, Shan Yang, Alexander C Berg, and Tamara L Berg. Modeling context in referring expressions. In *Eur. Conf. Comput. Vis.*, pages 69–85. Springer, 2016. 1, 6, 7
- [47] Yan Zeng, Xinsong Zhang, and Hang Li. Multi-grained vision language pre-training: Aligning texts with visual concepts. *arXiv preprint arXiv:2111.08276*, 2021. 2
- [48] Yunan Zeng, Yan Huang, Jinjin Zhang, Zequn Jie, Zhenhua Chai, and Liang Wang. Investigating compositional challenges in vision-language models for visual grounding. In *IEEE Conf. Comput. Vis. Pattern Recog.*, pages 14141–14151, 2024. 3, 7
- [49] Jianming Zhang, Zhe Lin, Jonathan Brandt, Xiaohui Shen, and Stan Sclaroff. Top-down neural attention by excitation backprop. In *Eur. Conf. Comput. Vis.*, 2016. 6
- [50] Yuxuan Zhang, Tianheng Cheng, Rui Hu, Lei Liu, Heng Liu, Longjin Ran, Xiaoxin Chen, Wenyu Liu, and Xinggang Wang. Evf-sam: Early vision-language fusion for text-prompted segment anything model. *arXiv preprint arXiv:2406.20076*, 2024. 7

- [51] Zheng Zhang, Yeyao Ma, Enming Zhang, and Xiang Bai. Psalm: Pixelwise segmentation with large multi-modal model. In *Eur. Conf. Comput. Vis.*, pages 74–91. Springer, 2025. [7](#)